

SANDIA REPORT

SAND2017-2998
Unlimited Release
Printed March 2017

Methodology for assessing the safety of Hydrogen Systems: HyRAM 1.1 technical reference manual

Katrina M. Groth, Ethan S. Hecht, John T. Reynolds, Myra L. Blaylock, Erin E. Carrier

Prepared by
Sandia National Laboratories
Albuquerque, New Mexico 87185 and Livermore, California 94550

Sandia National Laboratories is a multi-mission laboratory managed and operated by Sandia Corporation, a wholly owned subsidiary of Lockheed Martin Corporation, for the U.S. Department of Energy's National Nuclear Security Administration under contract DE-AC04-94AL85000.

Approved for public release; further dissemination unlimited.



Sandia National Laboratories

Issued by Sandia National Laboratories, operated for the United States Department of Energy by Sandia Corporation.

NOTICE: This report was prepared as an account of work sponsored by an agency of the United States Government. Neither the United States Government, nor any agency thereof, nor any of their employees, nor any of their contractors, subcontractors, or their employees, make any warranty, express or implied, or assume any legal liability or responsibility for the accuracy, completeness, or usefulness of any information, apparatus, product, or process disclosed, or represent that its use would not infringe privately owned rights. Reference herein to any specific commercial product, process, or service by trade name, trademark, manufacturer, or otherwise, does not necessarily constitute or imply its endorsement, recommendation, or favoring by the United States Government, any agency thereof, or any of their contractors or subcontractors. The views and opinions expressed herein do not necessarily state or reflect those of the United States Government, any agency thereof, or any of their contractors.

Printed in the United States of America. This report has been reproduced directly from the best available copy.

Available to DOE and DOE contractors from
U.S. Department of Energy
Office of Scientific and Technical Information
P.O. Box 62
Oak Ridge, TN 37831

Telephone: (865) 576-8401
Facsimile: (865) 576-5728
E-Mail: reports@adonis.osti.gov
Online ordering: <http://www.osti.gov/bridge>

Available to the public from
U.S. Department of Commerce
National Technical Information Service
5285 Port Royal Rd
Springfield, VA 22161

Telephone: (800) 553-6847
Facsimile: (703) 605-6900
E-Mail: orders@ntis.fedworld.gov
Online ordering: <http://www.ntis.gov/help/ordermethods.asp?loc=7-4-0#online>



Methodology for assessing the safety of Hydrogen Systems: HyRAM 1.1 technical reference manual

Katrina M. Groth
Risk & Reliability Analysis
Sandia National Laboratories
P.O. Box 5800, MS0748
Albuquerque, NM 87185

Ethan S. Hecht
Hydrogen & Materials Science
Sandia National Laboratories
7011 East Avenue, MS 9052
Livermore, CA 94550

John T. Reynolds
Mission Computing Services
Science Applications International Corporation
P.O. Box 5800, MS0748
Albuquerque, NM 87185

Myra L. Blaylock
Thermal/Fluid Science & Engineering
Sandia National Laboratories
7011 East Avenue, MS 9957
Livermore, CA 94550

Erin E. Carrier
Risk & Reliability Analysis
Sandia National Laboratories
P.O. Box 5800, MS0748
Albuquerque, NM 87185

Abstract

The HyRAM software toolkit provides a basis for conducting quantitative risk assessment and consequence modeling for hydrogen infrastructure and transportation systems. HyRAM is designed to facilitate the use of state-of-the-art science and engineering models to conduct robust, repeatable assessments of hydrogen safety, hazards, and risk. HyRAM is envisioned as a unifying platform combining validated, analytical models of hydrogen behavior, a standardized, transparent QRA approach, and engineering models and generic data for hydrogen installations. HyRAM is being developed at Sandia National Laboratories for the U. S. Department of Energy to increase access to technical data about hydrogen safety and to enable

the use of that data to support development and revision of national and international codes and standards.

This document provides a description of the methodology and models contained in the HyRAM version 1.1. HyRAM 1.1 includes generic probabilities for hydrogen equipment failures, probabilistic models for the impact of heat flux on humans and structures, and computationally and experimentally validated analytical and first order models of hydrogen release and flame physics. HyRAM 1.1 integrates deterministic and probabilistic models for quantifying accident scenarios, predicting physical effects, and characterizing hydrogen hazards (thermal effects from jet fires, overpressure effects from deflagrations), and assessing impact on people and structures. HyRAM is a prototype software in active development and thus the models and data may change. This report will be updated at appropriate developmental intervals.

Acknowledgment

The authors gratefully acknowledge the many productive discussions with the various stakeholders who have provided insight for this work. This research was supported by the U. S. Department of Energy (DOE), Office of Energy Efficiency, Fuel Cell Technologies Office. The authors gratefully acknowledge the support of DOE FCTO Safety Codes and Standards program manager Will James, Jay Keller, and Sandia colleagues Chris LaFleur, Alice Muna, Isaac Ekoto, Brian Somerday, Cathy Ottinger Farnum, Brian Ehrhart, Chris San Marchi and Jon Zimmerman. We also thank the members of: IEA HIA Task 37, ISO TC197 WG24, NFPA 2, the Hydrogen Safety Panel, and HySafe for engaging technical discussions and thoughtful feedback.

Contents

1	Introduction	11
1.1	About HyRAM and This Report	11
1.2	Background and Motivation	11
1.3	Design Goals and Limitations	12
1.4	Requirements	13
1.5	Summary of HyRAM Outputs	13
2	Quantitative Risk Assessment Methodology	15
2.1	Quantitative Risk Assessment Methodology Overview	15
2.2	Risk Metrics Calculations	15
2.3	Scenario Models	17
2.4	Frequency of a Gaseous Hydrogen Release	18
2.5	Consequence Models	19
2.5.1	Jet Fire	19
2.5.2	Explosion (Deflagration or Detonation) Overpressure	19
2.6	Harm and Loss Models	19
3	Default Frequency and Probability Data	23
3.1	Release Detection and Isolation Probability	23
3.2	Ignition Probabilities	23
3.3	Probability of Flash Fire vs. Explosion	23
3.4	Component Leak Frequencies	23
4	Physics Models.....	25
4.1	Properties of Hydrogen	25
4.1.1	Abel-Noble Equation of State	25
4.1.2	REFPROP Equation of State	27
4.2	Unignited Releases.....	28
4.2.1	Orifice Flow	28
4.2.2	Notional Nozzles	29
4.2.3	Gas Jet/Plume	30
4.2.4	Accumulation in Confined Areas/Enclosures	33
4.3	Ignited Releases	33
4.3.1	Jet Flame Without Buoyancy Correction	33
4.3.2	Jet Flame with Buoyancy Correction	35
4.3.3	Overpressure in Enclosures	37
5	Mathematics Middleware.....	39
5.1	The Math.NET Numerics Package	39
5.2	The HyRAM Unit Conversion System	39
6	Summary of Numerical Methods.....	41
6.1	Equation of State Computations	41
6.2	Notional Nozzle Model Computations	41

6.3	Unignited Gas/Jet Plume	41
6.4	Jet Flame	42
6.5	Overpressure	42
7	Engineering Toolkit	43
7.1	Temperature, Pressure, and Density	43
7.2	Tank Mass	43
7.3	Mass Flow Rate	43
7.4	TNT Mass Equivalence	44
	References	45

Figures

1	Summary of QRA methodology implemented in HyRAM toolkit.	16
2	Event Sequence Diagram for GH ₂ releases	18
3	Comparison of equations of state used in hydrogen modeling.	27
4	Sketch of plume model coordinates. Gravity acts in the negative y-direction.	31

Tables

1	Gaseous release scenarios modeled in HyRAM.	17
2	Probit models used to calculate fatality probability as a function of thermal dose (V). 20	
3	Probit models to calculate fatality probability from exposure to overpressures, where P_s is peak overpressure (Pa) and i is the impulse of the shock wave (Pa-s).	21
4	Parameters for frequency of random leaks for individual components	24
5	HyRAM Convertible Units	40

Nomenclature

AIR Average Individual Risk

API Application Program Interface

BLAS Basic Linear Algebra Subprograms

BSD Berkeley Software Distribution

DOE U. S. Department of Energy

EERE Office of Energy Efficiency and Renewable Energy

ESD Event Sequence Diagram

FAR Fatal Accident Rate

FCTO Fuel Cell Technologies Office

FT Fault Tree

GH₂ Gaseous Hydrogen

H₂ Hydrogen

HIA Hydrogen Implementing Agreement

HyRAM Hydrogen Risk Assessment Models

IEA International Energy Agency

ISO International Organization for Standardization

LAPACK Linear Algebra Package

LU Lower Upper

NFPA National Fire Protection Association

NIST National Institute of Standards and Technology

ODE Ordinary Differential Equation

PLL Potential Loss of Life

QRA Quantitative Risk Assessment

SI International System of Units

SNL Sandia National Laboratories

TNT Trinitrotoluene

1 Introduction

1.1 About HyRAM and This Report

HyRAM (Hydrogen Risk Assessment Models) is a prototype software toolkit that integrates data and methods relevant to assessing the safety of hydrogen fueling and storage infrastructure. The HyRAM toolkit integrates deterministic and probabilistic models for quantifying accident scenarios, predicting physical effects, and characterizing the impact of hydrogen hazards, including thermal effects from jet fires and overpressure effects from deflagration in enclosures. HyRAM incorporates generic probabilities for equipment failures for nine types of components, and probabilistic models for the effect of heat flux and overpressure on humans and structures. HyRAM also incorporates computationally and experimentally validated models of various aspects of hydrogen release and flame physics. HyRAM can be used to support multiple types of analysis, including code and standards development, safety basis development, and facility safety planning.

HyRAM provides a platform which integrates state-of-the-art, validated science and engineering models and data relevant to hydrogen safety into a comprehensive, industry-focused platform. The use of a standard platform for conducting hydrogen Quantitative Risk Assessment (QRA) ensures that various industry stakeholders can produce repeatable, verifiable results. HyRAM is designed in a modular configuration that will permit revision of individual modules using advances in scientific understanding and engineering basis of hydrogen systems.

HyRAM was developed by Sandia National Laboratories (SNL) for the U.S. Department of Energy's Office of Energy Efficiency and Renewable Energy (EERE) Fuel Cell Technologies Office (FCTO). The hydrogen gas release and jet flame models used in the HyRAM platform have been validated against available experimental and computational data for hydrogen in the parameter range of interest for hydrogen transportation systems. The probability data encoded in HyRAM have been developed by reference to published hydrogen data. In the future, HyRAM will be extended in scope and depth via user-contributed models and data.

This report provides technical documentation of the algorithms, models, and data incorporated in HyRAM 1.1. Additional technical information can be found in the HyRAM conference papers [1–3] and in the references cited in this report. User guidance can be found in [4] and HyRAM testing strategy is discussed in [5]. Additional documentation, including software design and Application Program Interface (API) information, and model validation information, will be generated at appropriate development intervals. HyRAM 1.1 is a prototype software and as such the models and data in HyRAM may change. Software documentation will be revised as new versions are developed.

1.2 Background and Motivation

Hydrogen fuels for the transportation sector are being deployed around the world as an alternative to traditional petrol and battery technologies. As with all fuels, regulations, codes and standards

are a necessary component of the safe deployment of hydrogen technologies. There has been a focused effort in the international hydrogen community to develop codes and standards based on strong scientific principles to accommodate the relatively rapid deployment of hydrogen-energy systems.

Both QRA and deterministic hydrogen behavior modeling have become valuable tools for the development and revision of hydrogen codes and standards such as NFPA 2, NFPA 55, and ISO TR-19880 [6–12]. However, the use of QRA in hydrogen applications currently suffers from limitations and inefficiency due to a range of factors, including wide variation in QRA and consequence modeling approaches, the use of unvalidated physics models, lack of data, and more [2, 13–17].

The FCTO and SNL initiated the development of HyRAM to enable code development committees to conduct QRA, hazard, and consequence analyses using a fast-running, comprehensive methodology based in science and engineering models from the hydrogen safety research community [1, 2]. The HyRAM software toolkit establishes a common methodology for conducting QRA with integrated reduced-order physical models. Establishing a consistent, documented methodology and corresponding software toolkit facilitates comparison of results between different stakeholders.

1.3 Design Goals and Limitations

HyRAM is designed to calculate multiple risk and harm/damage metrics from user-defined system configurations to provide insights for decision makers in the codes and standards community. HyRAM contains generic information and fast-running, analytical, and first-order models designed to facilitate comparison of different system designs and requirements. As such, the focus of HyRAM is on enabling systematic, rigorous risk comparison and sensitivity analysis rather than on establishing the “true” frequency of a hypothetical accident. HyRAM is designed to produce realistic best estimates for use in decision-making.

Note: Risk and safety assessment results should be used as part of a decision process, not as the sole basis for a decision. Safety and design decisions involve consideration of many factors and judgments; these factors include the safety assessments, the assumptions and limitations of safety assessments, the benefits of a technology, and public preferences. As such, HyRAM does not allow the user to specify an acceptability or tolerability criteria for risk or harm. Further guidance on QRA and tolerability criteria can be found in the references [18–24].

HyRAM is designed to enable defensible, repeatable calculations using consistent, documented algorithms. The algorithms, models, and data in HyRAM have been assembled from published, publicly available sources. The physics models contained in HyRAM have been validated through a combination of experimental and simulation activities. Where model validation is not possible (e.g., for harm models), HyRAM is designed to allow users to choose among different models. HyRAM includes generic data for hydrogen component leak frequencies and documented, expert-assigned probabilities for ignition. HyRAM is designed to allow users to replace the default data and assumptions with system-specific information when such information is available to the user.

1.4 Requirements

HyRAM was designed to be installed on any 32-or-64-bit Intel-compatible computer with more than 4GB/RAM and 4GB free persistent storage (hard drive space), running Microsoft Windows 98 or later.

HyRAM is a software prototype under active development provided as-is.

1.5 Summary of HyRAM Outputs

The QRA mode in HyRAM can be used to calculate several risk metrics. The HyRAM toolkit includes three well-known risk metrics which are commonly used to evaluate fatality risk in multiple industries, as well as several additional risk metrics:

- FAR (Fatal Accident Rate) the expected number of fatalities in 100 million exposed hours;
- AIR (Average Individual Risk) the expected number of fatalities per exposed individual;
- PLL (Potential Loss of Life) the expected number of fatalities per system-year;
- Expected number of hydrogen releases per system-year (unignited and ignited cases);
- Expected number of jet fires per system-year (immediate ignition cases);
- Expected number of deflagrations/explosions per system-year (delayed ignition cases).

The physics mode of HyRAM can be used to calculate multiple physical effects associated with hydrogen, including:

- Jet flame temperature at user-defined positions;
- Jet flame radiative heat flux (kW/m^2) at user-defined positions;
- 3D plots (isometric contours) of distance to user-defined heat flux levels from jet flames;
- Overpressure due to accumulation and delayed ignition in an enclosure.

2 Quantitative Risk Assessment Methodology

2.1 Quantitative Risk Assessment Methodology Overview

In quantitative risk assessment, multiple integrated models are used to provide a framework for reasoning about decision options, based on the background information encoded in those models.

Risk is characterized by a set of hazard exposure scenarios (i), the consequences (c_i) associated with each scenario, and the probability of occurrence (p_i) of these consequences. One commonly used expression for calculating risk is:

$$\text{Risk} = \sum_i (p_i \times c_i) \quad (1)$$

In QRA, the consequences are expressed in terms of an observable quantity, such as number of fatalities or repair cost in a specific period of time. The probability term expresses the analysts' uncertainty about predicted consequences (which encompasses the frequency of different scenarios and the range of possible consequences for each scenario).

The major elements of the QRA methodology in HyRAM are shown in Figure 1.

2.2 Risk Metrics Calculations

The Fatal Accident Rate (FAR) and Average Individual Risk (AIR) are commonly used metrics for expressing the fatality risk for a platform. FAR and AIR are expressed as a function of the Potential Loss of Life (PLL). The PLL expresses the expected number of fatalities, per system-year. PLL is expressed as follows:

$$\text{PLL} = \sum_n (f_n \times c_n) \quad (2)$$

where n is one of the possible safety-significant scenarios (described in Section 2.3), f_n is the frequency of that accident scenario n (described in Sections 2.3 and 2.4), and c_n is the expected number of fatalities for accident scenario n (described in Section 2.6).

The FAR is the expected number of fatalities in a group, per 100 million exposed hours. The FAR for a particular facility can be calculated using the PLL, as well as the population of the facility. FAR is calculated using Equation 3.

$$\text{FAR} = \frac{\text{PLL} \times 10^8}{\text{Exposed hours}} = \frac{\text{PLL} \times 10^8}{N_{\text{pop}} \times 8760} \quad (3)$$

where N_{pop} is the average number of personnel in the facility, and dividing by 8760 converts from years to hours.

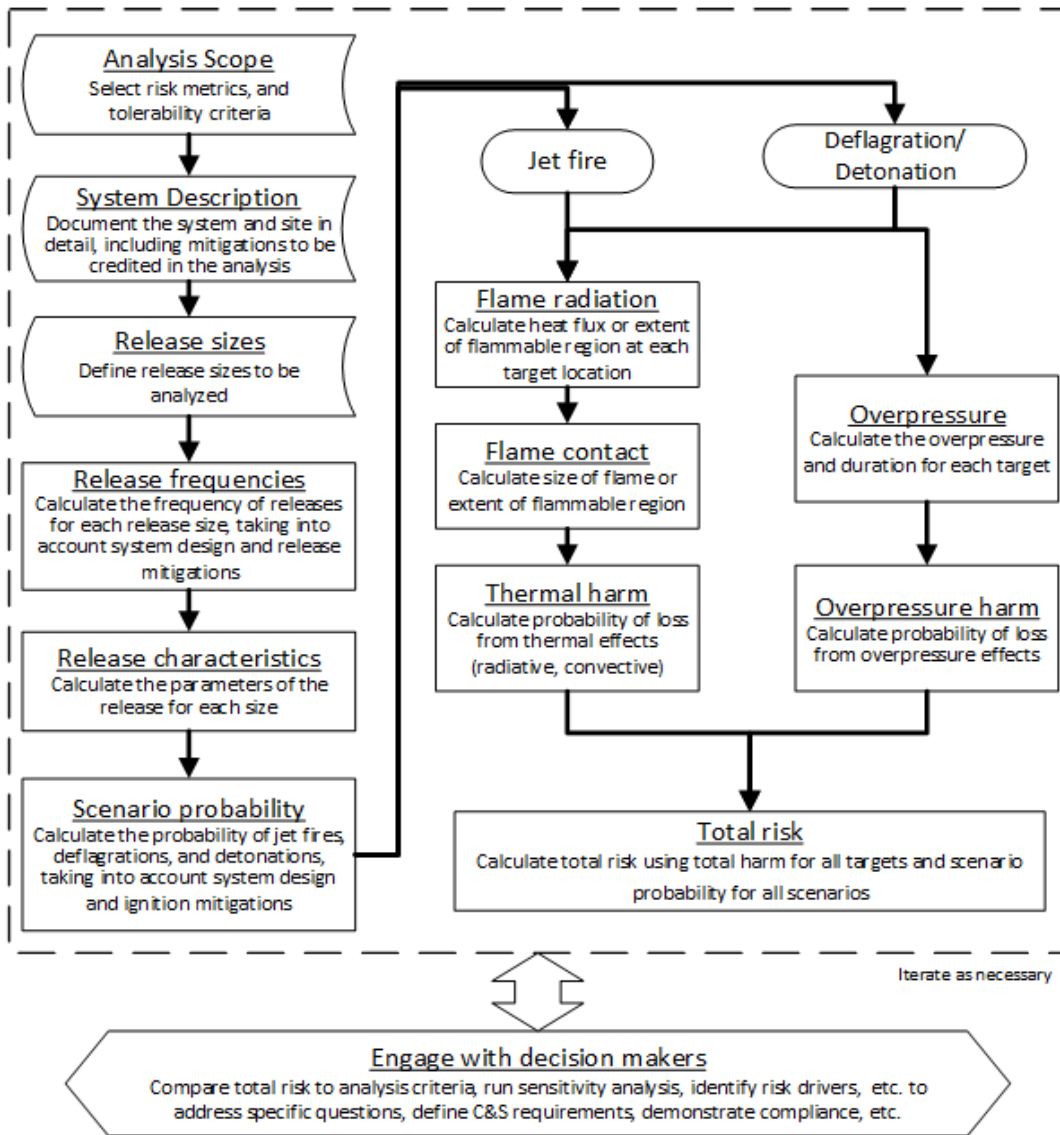


Figure 1. Summary of QRA methodology implemented in HyRAM toolkit.

The AIR expresses the average number of fatalities per exposed individual. It is based on the number of hours the average occupant spends at the facility.

$$\text{AIR} = H \times \text{FAR} \times 10^{-8} \quad (4)$$

where H is the annual number of hours the individual spends in the facility (e.g., 2000 hours for full-time worker).

2.3 Scenario Models

A release of hydrogen could lead to several different physical consequences and associated hazards. For continuous releases of gaseous hydrogen, the physical consequences are unignited releases, jet fires (thermal effects), flash fires (deflagration of accumulated gas, dominated by thermal effects) and explosions (deflagration or detonation of accumulated gas dominated by overpressure effects). Table 1 describes the pivotal events and combustion associated with each physical consequence, as well as which hazard is modeled in HyRAM.

Table 1. Gaseous release scenarios modeled in HyRAM.

Physical conseq.	Pivotal Events	Combustion description	Hazard
Jet fire	Continuous release (i.e., until H ₂ supply is exhausted); immediate ignition	A non-premixed turbulent flame, momentum driven. The speed of the combustion is roughly equal to the gas release rate.	Thermal effects
Flash fire	Deflagration of accumulated gas, delayed ignition (i.e., ignition occurs after accumulation and mixing)	A premixed flame burning faster than H ₂ is being released/added to the mixture.	Thermal effects
Explosion	Deflagration or detonation of accumulated gas, delayed ignition	Rapid flame propagation in a confined area (detonations also result in a shock wave)	Overpressure effects

These scenarios are modeled in the Event Sequences Diagram (ESD) for release of gaseous hydrogen (see Figure 2). The ESD is encoded in HyRAM using the following equations¹:

$$f_{\text{Unignited}} = f_{\text{GH2 Release}} \times P(\text{Isolated}) \quad (5)$$

$$+ f_{\text{GH2 Release}} \times P(\overline{\text{Isolated}}) \times P(\overline{\text{Immed. Ignite}}) \times P(\overline{\text{Delayed Ignite}})$$

$$f_{\text{Jetfire}} = f_{\text{GH2 Release}} \times P(\overline{\text{Isolated}}) \times P(\text{Immed. Ignite}) \quad (6)$$

$$f_{\text{Flashfire}} = f_{\text{GH2 Release}} \times P(\overline{\text{Isolated}}) \times P(\overline{\text{Immed. Ignite}}) \times P(\text{Delayed Ignite}) \times P(\text{TvsP}) \quad (7)$$

$$f_{\text{Explosion}} = f_{\text{GH2 Release}} \times P(\overline{\text{Isolated}}) \times P(\text{Immed. Ignite}) \times P(\text{Delayed Ignite}) \times P(\overline{\text{TvsP}}) \quad (8)$$

where $f_{\text{GH2 Release}}$ is the annual frequency of a gaseous hydrogen release, (see Section 2.4), $P(\text{Isolated})$ is the probability of release (leak) detection and isolation before ignition, $P(\text{Immed. Ignite})$ is the probability of immediate ignition, $P(\text{Delayed Ignite})$ is the probability of delayed ignition (see Section 3), and $P(\text{TvsP})$ is the probability that the dominant effects from the ignition of accumulated gas are thermal (rather than overpressure) (see Section 3).

¹Notation: $P(\text{event})$ is the probability of occurrence of the event; $P(\overline{\text{event}})$ means the probability of non-occurrence of an event, which is equal to $P(\overline{\text{event}}) = 1 - P(\text{event})$

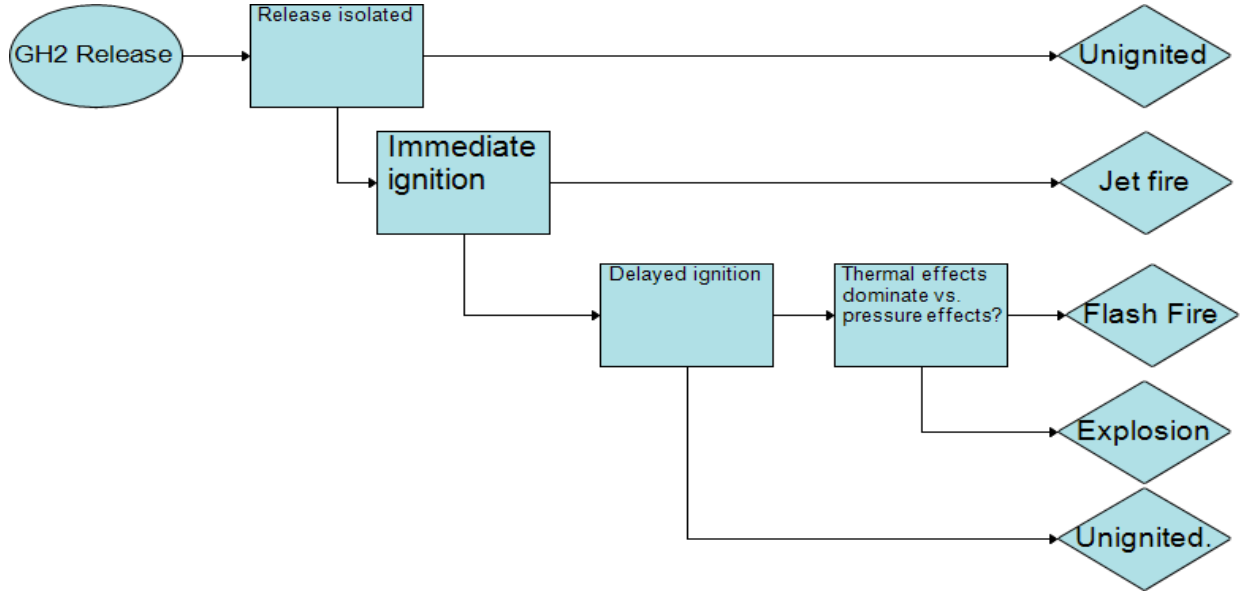


Figure 2. Event Sequence Diagram for GH₂ releases

2.4 Frequency of a Gaseous Hydrogen Release

$f_{\text{GH2 Release}}$ is a vector of the annual frequency of a gaseous hydrogen releases (of sizes, k , 0.01%, 0.1%, 1%, 10%, 100% of pipe flow area, $\frac{\pi}{4}d^2$, where d is the inner diameter of the pipe²).

HyRAM calculates the annual frequency of a gaseous hydrogen release for 0.01%, 0.1%, 1%, 10% (using (9)), 100% (using (10)) releases using the following equations:

$$f_{\text{GH2 Release}} = f_{\text{Random Releases}} \quad (9)$$

$$f_{\text{GH2 Release}} = f_{\text{Random Releases}} + f_{\text{Other Releases}} \text{ (100\% releases only)} \quad (10)$$

where $f_{\text{Random Releases}}$ is obtained from the parts count approach:

$$f_{\text{Release of size } k} = \sum_i N_{\text{Component}_i} \times f_{\text{Leak}_{i,k}} \quad (11)$$

Where $N_{\text{Component}_i}$ is user input for the number of components of each of nine types (Compressors, Cylinders, Valves, Instruments, Joints, Hoses, Pipes (m), Filters, Flanges), and f_{Leak_i} is the mean leak frequency of size k for component i (see Section 3).

$f_{\text{Other Releases}}$ is a placeholder for future HyRAM modules (a planned Fault Tree editor). In HyRAM 1.1, this value comes from a hard-coded probability, which produces results as follows:

$$f_{\text{Other Releases}} = 5.5 \times 10^{-9} \times (n_{\text{Demands per Day}} \times n_{\text{Operating Days}}) \quad (12)$$

²The discharge coefficient used in QRA mode is 1.0. This default cannot currently be changed.

Where the user enters the following parameters: the number of times per day that the system is used ($n_{\text{Demands per Day}}$), and the number of system operating days per year ($n_{\text{Operating Days}}$).

2.5 Consequence Models

2.5.1 Jet Fire

The consequences of a jet fire (for each of the five release sizes) are calculated using the models described in Section 4. Users have two choices of jet flame models: the models of Houf and Schefer [25] as described in Section 4.3.1, and the models from Ekoto et al. [26] as described in Section 4.3.2. Both of these models are coupled to the orifice flow and notional nozzle models described in Section 4.2. The discharge coefficient C_d is set to 1.0.

The target positions (x, y, z) are converted to distances relative to the flame (x, r) and are defined by user input or random sampling. Users assign a number of targets. For each target, the user may assign a position deterministically or may use a probability distribution to be randomly sampled to assign the positions. Currently users may select a normal or uniform distribution as described in Section 5.1.

2.5.2 Explosion (Deflagration or Detonation) Overpressure

HyRAM V1.1 requires user input for the overpressure consequences (for either confined or unconfined situations). Users must input the peak overpressure and impulse (e.g., from calculations using computational simulation, first-order models, or engineering assumptions) for the five release sizes. Users should note that ignition of unconfined hydrogen is unlikely to generate significant overpressures due to buoyancy of hydrogen. For overpressures in enclosures/with confinement, these may be calculated using the overpressure model in HyRAM physics mode (see Section 4.3.3). Subsequent versions of HyRAM will hook the overpressure model into QRA mode.

2.6 Harm and Loss Models

Probit models are used to establish the probability of injury or fatality for a given exposure. The probit model is a linear combination of predictors that model the inverse cumulative distribution function associated with the normal distribution³. The probability of a fatality is given by Equation 13, which evaluates the normal cumulative distribution function, Φ , at the value established by the probit model (Y); this is accomplished using the Math.NET numerics package (Section 5). Different probit models for thermal and overpressure effects are discussed in the following subsections.

³Today, probit model are associated with the standard normal distribution, with mean $\mu = 0$ and standard deviation $\sigma = 1$. Some older probit models were developed using $\mu = 5$ to avoid negative values. We use $\mu = 5$ to be consistent with the published fatality probit models.

Table 2. Probit models used to calculate fatality probability as a function of thermal dose (V).

Reference	Fatality Model	Notes
Eisenberg [28]	$Y = -38.48 + 2.56 \times \ln(V)$	Based on population data from nuclear blasts at Hiroshima and Nagasaki (ultra-violet radiation)
Tsao & Perry [29]	$Y = -36.38 + 2.56 \times \ln(V)$	Eisenberg model, modified to account for infrared radiation
TNO [30]	$Y = -37.23 + 2.56 \times \ln(V)$	Tsao and Perry model modified to account for clothing
Lees [31]	$Y = -29.02 + 1.99 \times \ln(0.5V)$	Accounts for clothing, based on porcine skin experiments using ultraviolet source to determine skin damages. Uses burn mortality information.

$$P(\text{fatality}) = F(Y|\mu, \sigma) = \Phi(Y - 5) \quad (13)$$

Thermal Harm For thermal radiation, the harm level is a function of both the heat flux intensity and the duration of exposure. Harm from radiant heat fluxes is often expressed in terms of a thermal dose unit which combines the heat flux intensity and exposure time by Equation 14:

$$\text{Thermal Dose Unit} = V = I^{(4/3)} \times t \quad (14)$$

where I is the radiant heat flux in W/m^2 and t is the exposure duration in seconds. The default thermal exposure time used in HyRAM is 60 s – users may modify this value.

Table 2 lists five thermal probit models that are encoded in HyRAM. The probability of a fatality is evaluated by inserting the probit model from Table 2 into Equation 13. LaChance et al. [27] recommend using both the Eisenberg and the Tsao & Perry probit models for hydrogen-related applications.

Structures and equipment can also be damaged by exposure to radiant heat flux. Some typical heat flux values and exposure times for damage to structures and components were provided by LaChance et al. [27]. However, because the exposure times required for damage is long ($> 30\text{min}$), the impact of thermal radiation from hydrogen fires on structures and equipment is not generally significant since personnel are able to evacuate the building before significant structural damage occurs.

Overpressure Harm There are several probit models available to predict harm and loss from blast overpressures. These models generally differential between direct effects of pressure and indirect effects. Significant increases in pressure can cause damage to pressure-sensitive organs such

Table 3. Probit models to calculate fatality probability from exposure to overpressures, where P_s is peak overpressure (Pa) and i is the impulse of the shock wave (Pa-s).

Reference	Fatality model
Eisenberg - Lung hemorrhage [18]	$Y = -77.1 + 6.91 \ln(P_s)$
HSE - Lung hemorrhage [32]	$Y = 1.47 + 1.371 \ln(P_s)$
TNO - Head impact [30]	$Y = 5 - 8.49 \ln((2430/P_s) + 4.0 \times 10^8/(P_s i))$
TNO - Structure collapse [30]	$Y = 5 - 0.22 \ln(V)$ Where $V = (40000/P_s)^{7.4} + (460/i)^{11.3}$

as the lungs and ears. Indirect effects include the impact from fragments and debris generated by the overpressure event, collapse of structures, and heat radiation (e.g., from the fireball generated during a vapor cloud explosion). Large explosions can also carry a person some distance resulting in injury from collisions with structures or from the resulting violent movement. The probit models for the effects of overpressures that are included in HyRAM are provided in Table 3.

LaChance et al. [27] recommend the use of the TNO probit models, and suggests that indirect effects from overpressure events represent the most important concern for people. The overpressures required to cause fatal lung damage are significantly higher than the values required to throw a person against obstacles or to generate missiles that can penetrate the skin. In addition, a person inside a structure would more likely be killed by the facility collapse than from lung damage. For this reason, we use the TNO probit model for structural collapse in this analysis.

3 Default Frequency and Probability Data

3.1 Release Detection and Isolation Probability

The default value for successful detection and isolation of a release, $P(\text{Isolate})$, is 0.9.

3.2 Ignition Probabilities

The default hydrogen ignition probabilities are a function of hydrogen release rate; these values come from [17].

Hydrogen release rate (kg/s)	$P(\text{Immediate Ignition})$	$P(\text{Delayed Ignition})$
<0.125	0.008	0.004
0.125 - 6.25	0.053	0.027
>6.25	0.230	0.120

3.3 Probability of Flash Fire vs. Explosion

The pivotal event *thermal effects dominate vs. pressure effects* denotes the probability of an accumulated gas fire leading to a flash fire flash fire with no pressure effects. The complement event denotes the probability of leading to an explosion with pressure effects⁴.

In HyRAM 1.1, the probability for this event is 0.0 (due to ongoing development of the thermal consequence models). In a future version of HyRAM, this probability will be changed to a default probability of 0.6 once the layer consequence model is integrated into QRA mode.

3.4 Component Leak Frequencies

In HyRAM 1.1, the mean leak frequency is used in release calculations. Future versions of HyRAM will be designed to use additional information from the lognormal distribution in uncertainty propagation.

The frequency of a random leak (release) is calculated from the parameters of a lognormal distribution (μ , σ). The default values are generic hydrogen-system leak frequencies developed by [7] are found in Table 4. HyRAM calculates the mean and variance from the values μ and σ using the properties of the lognormal distribution: mean = $e^{\mu+\sigma^2/2}$, variance = $(e^{\sigma^2} - 1)e^{2\mu+\sigma^2}$.

⁴Note: some QRA approaches require and model the opposite assumption about the occurrence of an explosion – this probability should be subtracted from 1 and used in this variable

Table 4. Parameters for frequency of random leaks for individual components

Component	Release size	μ	σ	Mean (Calculated)	Variance (Calculated)
Compressors	0.01%	-1.72	0.21	1.83×10^{-1}	1.58×10^{-3}
	0.1%	-3.92	0.48	2.23×10^{-2}	1.32×10^{-4}
	1%	-5.14	0.79	8.01×10^{-3}	5.55×10^{-5}
	10%	-8.84	0.84	2.06×10^{-4}	4.31×10^{-8}
	100%	-11.34	1.37	3.04×10^{-5}	5.11×10^{-9}
Cylinders	0.01%	-13.84	0.62	1.18×10^{-6}	6.46×10^{-13}
	0.1%	-14.00	0.61	9.98×10^{-7}	4.43×10^{-13}
	1%	-14.40	0.62	6.80×10^{-7}	2.19×10^{-13}
	10%	-14.96	0.63	3.90×10^{-7}	7.36×10^{-14}
	100%	-15.60	0.67	2.09×10^{-7}	2.47×10^{-14}
Filters	0.01%	-5.25	1.98	3.77×10^{-2}	7.18×10^{-2}
	0.1%	-5.29	1.52	1.60×10^{-2}	2.30×10^{-3}
	1%	-5.34	1.48	1.44×10^{-2}	1.64×10^{-3}
	10%	-5.38	0.89	6.87×10^{-3}	5.67×10^{-5}
	100%	-5.43	0.95	6.94×10^{-3}	7.16×10^{-5}
Flanges	0.01%	-3.92	1.66	7.86×10^{-2}	9.13×10^{-2}
	0.1%	-6.12	1.25	4.82×10^{-3}	8.84×10^{-5}
	1%	-8.33	2.20	2.72×10^{-3}	9.41×10^{-4}
	10%	-10.54	0.83	3.74×10^{-5}	1.41×10^{-9}
	100%	-12.75	1.83	1.55×10^{-5}	6.53×10^{-9}
Hoses	0.01%	-6.81	0.27	1.15×10^{-3}	9.82×10^{-8}
	0.1%	-8.64	0.55	2.06×10^{-4}	1.51×10^{-8}
	1%	-8.77	0.54	1.79×10^{-4}	1.11×10^{-8}
	10%	-8.89	0.55	1.60×10^{-4}	8.92×10^{-9}
	100%	-9.86	0.85	7.47×10^{-5}	5.82×10^{-9}
Joints	0.01%	-9.57	0.16	7.05×10^{-5}	1.35×10^{-10}
	0.1%	-12.83	0.76	3.56×10^{-6}	9.84×10^{-12}
	1%	-11.87	0.48	7.80×10^{-6}	1.54×10^{-11}
	10%	-12.02	0.53	6.96×10^{-6}	1.57×10^{-11}
	100%	-12.15	0.57	6.21×10^{-6}	1.45×10^{-11}
Pipes	0.01%	-11.86	0.66	8.78×10^{-6}	4.16×10^{-11}
	0.1%	-12.53	0.69	4.57×10^{-6}	1.26×10^{-11}
	1%	-13.87	1.13	1.80×10^{-6}	8.27×10^{-12}
	10%	-14.58	1.16	9.12×10^{-7}	2.33×10^{-12}
	100%	-15.73	1.71	6.43×10^{-7}	7.39×10^{-12}
Valves	0.01%	-5.18	0.17	5.71×10^{-3}	9.90×10^{-7}
	0.1%	-7.27	0.40	7.50×10^{-4}	9.67×10^{-8}
	1%	-9.68	0.96	9.92×10^{-5}	1.49×10^{-8}
	10%	-10.32	0.68	4.13×10^{-5}	9.86×10^{-10}
	100%	-12.00	1.33	1.49×10^{-5}	1.09×10^{-9}
Instruments	0.01%	-7.32	0.68	8.31×10^{-4}	4.00×10^{-7}
	0.1%	-8.50	0.79	2.78×10^{-4}	6.80×10^{-8}
	1%	-9.06	0.90	1.73×10^{-4}	3.68×10^{-8}
	10%	-9.17	1.07	1.84×10^{-4}	7.18×10^{-8}
	100%	-10.20	1.48	1.11×10^{-4}	9.85×10^{-8}

4 Physics Models

HyRAM includes a physics mode, which provides models relevant to modeling behavior, hazards, and consequences of hydrogen releases. Jet flames, concentration profiles for unignited jets/plumes, and indoor accumulation with delayed ignition causing overpressure can all be investigated from physics mode. A subset of these models is used in QRA mode to calculate the consequences from a given release scenario, as described in Section 2.5. Several basic property calculations (e.g., the thermodynamic equation of state for hydrogen) are necessary to numerically simulate hydrogen release scenarios, and these property calculations are used in many of the other models.

4.1 Properties of Hydrogen

The modules in this section provide thermodynamic properties of hydrogen gas and hydrogen releases, which are needed to calculate different aspects of hydrogen dispersion and combustion. These calculations are called from several of the other models. They are described here in detail, and then referred to in subsequent sections.

4.1.1 Abel-Noble Equation of State

Description: The Abel-Noble formulation provides a simple and accurate relationship between pressure, volume, and temperature for gaseous hydrogen and is more accurate than the ideal gas equation of state at high pressures characteristic of some hydrogen release scenarios. This section also includes thermodynamic relationships for isentropic expansion, as is often assumed during release scenarios. Deviations from the real hydrogen behavior become significant at cryogenic temperature.

Assumptions: Co-volume constant can account for intermolecular gas interactions.

Relationships: The equation of state can be written as

$$P = \frac{\frac{R}{M}\rho T}{1 - b\rho}, \quad (15)$$

where P is the pressure, R is the ideal gas constant, M is the molecular weight (2.016×10^{-3} m³/kg for H₂), ρ is the density, T is the temperature, and b is a co-volume constant (7.691×10^{-3} m³/kg for H₂) that accounts for intermolecular gas interactions. Note that this relationship becomes the ideal gas law if the co-volume constant is set to 0.

Using this relationship, and the Maxwell relationships, the density after an isentropic expansion can be calculated from the equality

$$\frac{\rho_0}{1 - b\rho_0} = \frac{\rho}{1 - b\rho} \left(1 + \frac{\gamma - 1}{2(1 - b\rho)^2} \text{Ma}^2 \right)^{\frac{1}{\gamma-1}}, \quad (16)$$

where the subscript 0 denotes stagnant conditions (before expansion), Ma is the Mach number ($\text{Ma} = v/a$, where v is the velocity and a is the speed of sound), and γ is the ratio of the heat capacities (c_p/c_v , which is 1.4 for hydrogen). Once the density after expansion is known, the temperature can be calculated through one of several equivalent relationships (depending on the known quantities):

$$T = T_0 \left(\frac{1 - b\rho_0}{\rho_0} \frac{\rho}{1 - b\rho} \right)^{\gamma-1}, \quad (17)$$

$$T = \frac{T_0}{1 + \left(\frac{\gamma-1}{2(1-b\rho)^2} \right) \text{Ma}^2}, \quad (18)$$

$$T = T_0 + \frac{b(P_0 - P) + (v_0^2 - v^2)/2}{c_p}, \quad (19)$$

where the heat capacity at constant pressure, $c_p = \frac{\gamma R/M}{\gamma-1}$. The final relationship that is needed is the speed of sound,

$$a = \frac{1}{1 - b\rho} \sqrt{\gamma \frac{R}{M} T}. \quad (20)$$

Applicability: The Abel-Nobel equation of state is accurate for hydrogen at pressures less than 200 MPa and temperatures greater than 150 K. Figure 3 shows the density of normal hydrogen, as calculated using the NIST Standard Reference Database 23 (REFPROP) [33, 34]. As shown in the top right frame, the Abel-Nobel equation of state, using the co-volume constant $b = 7.691 \times 10^{-3} \text{ m}^3/\text{kg}$ provides accurate predictions of density (within approximately 1%) in this range (which is grayed slightly in the plot, within the green portion in the lower right hand corner). As a comparison, the relative error in density for the ideal gas law ($b = 0$), is also shown in the lower right frame. The ideal gas law is valid up to approximately 5 MPa, at temperatures greater than 100 K. In the right hand side plots, the red portions indicate that the ideal gas law performs poorly at high pressures.

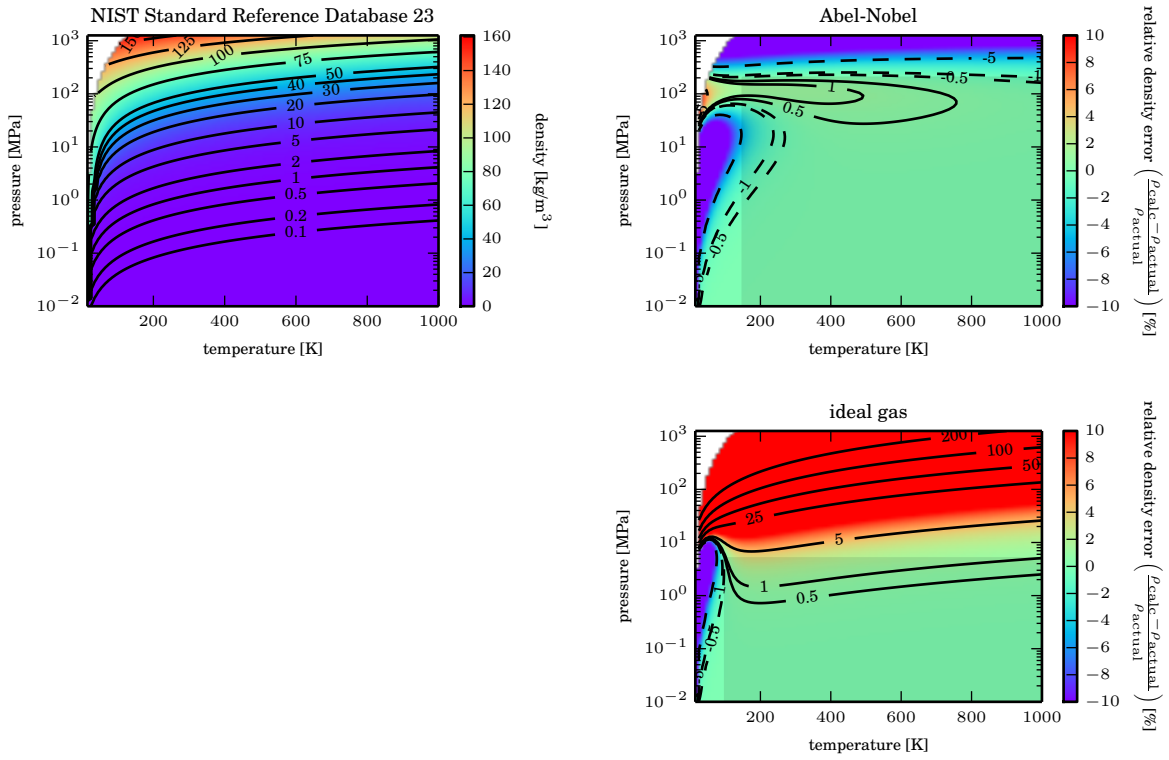


Figure 3. Comparison of equations of state used in hydrogen modeling. The top left plot shows the density of normal hydrogen, as calculated using the NIST Standard Reference Database 23 (REFPROP) [33, 34]. Top right plot shows the relative error in density calculated using the Abel-Nobel equation of state (Eq. 15). For comparison, the relative error using the ideal-gas law (Eq. 15 where $b = 0$) is shown in the bottom graphic. The region of validity for the Abel-Noble and ideal gas law is grayed slightly, within the green portion in the lower right hand corner, in both right-hand plots.

4.1.2 REFPROP Equation of State

Note: Use of REFPROP requires a REFPROP license and installation. REFPROP cannot be selected in the HyRAM 1.1 GUI. Hooks are being developed to enable REFPROP use in a future version of HyRAM.

Description: The NIST Standard Reference Database 23 (REFPROP) [33] is a robust thermodynamic calculator that is updated with the latest thermodynamic relationships for a wide range of materials. This module accounts for the real gas behavior of hydrogen at high pressure and at

cryogenic temperatures and is considered true thermodynamics of hydrogen. It can also be used to calculate the properties of air or other gases. For hydrogen, the relationships are detailed in Leachman et al. [34].

Relationships: REFPROP can be used to relate the pressure, temperature, density, enthalpy and entropy of a gas (when two of the thermodynamic quantities are known, all others can be calculated). One additional relationship is needed to calculate the thermodynamic state after isentropic expansion. If an expansion is isentropic, the initial entropy will be equal to the final entropy, and energy conservation requires

$$H_0 + \frac{v_0^2}{2} = H + \frac{v^2}{2}, \quad (21)$$

where H is the enthalpy of the system, v is the velocity, and the subscript 0 denotes stagnant conditions (before expansion).

Applicability: The REFPROP equation of state can be used for hydrogen that is less than 2000 MPa and between 14 K and 1000 K.

4.2 Unignited Releases

4.2.1 Orifice Flow

When the pressure ratio across an orifice is above the critical ratio (≈ 1.9 for hydrogen), the flow chokes, meaning that it is sonic, or flowing at the speed of sound through the throat, but remains at a higher pressure than the outlet pressure. The relationships described previously for isentropic expansion are used to calculate the flow rate through orifices, and the thermodynamic state in the throat. Orifices in HyRAM are assumed to be circular, characterized by their diameter, d , and a coefficient of discharge, C_d . The choked flow through any orifice can then be calculated as $\dot{m} = \pi/4 d^2 \rho v C_d$.

In the case of a storage tank with a given volume, the transient process of the tank emptying can also be calculated by HyRAM. In this case, a pseudo-steady-state is assumed, with a small time step (dt). The new total mass of hydrogen is calculated by $m - \dot{m} \cdot dt$. A new density is calculated using the new mass and tank volume. The temperature of the gas in the tank is recalculated assuming it expands isentropically to the new density (m/V , where V is the volume; see, for example Eq. 17). Iterations continue until the pressure in the tank is atmospheric. Generally, 1000 steps of equal mass flow are taken to empty the tank.

4.2.2 Notional Nozzles

Notional nozzles are used to calculate the effective diameter, velocity, and thermodynamic state after the complex shock structure of an under-expanded jet. They all conserve mass, with some also conserving momentum, and in some cases, other properties, are used across the shock to determine the conditions when the jet pressure is back to ambient.

Birch et al. [35] show that the conservation of mass

$$\rho_{\text{eff}} v_{\text{eff}} A_{\text{eff}} = \rho_{\text{throat}} v_{\text{throat}} A_{\text{throat}} C_D, \quad (22)$$

and momentum

$$\rho_{\text{eff}} v_{\text{eff}}^2 A_{\text{eff}} = \rho_{\text{throat}} v_{\text{throat}}^2 A_{\text{throat}} C_D + A_{\text{throat}} (P_{\text{throat}} - P_{\text{ambient}}), \quad (23)$$

can be solved for the effective velocity

$$v_{\text{eff}} = v_{\text{throat}} C_D + \frac{P_{\text{throat}} - P_{\text{ambient}}}{\rho_{\text{throat}} v_{\text{throat}} C_D}, \quad (24)$$

and the effective area

$$A_{\text{eff}} = \frac{\rho_{\text{throat}} v_{\text{throat}}^2 A_{\text{throat}} C_D^2}{\rho_{\text{eff}} (P_{\text{throat}} - P_{\text{ambient}} + \rho_{\text{throat}} v_{\text{throat}}^2 C_D^2)}, \quad (25)$$

where ρ is the density, v is the velocity, A is the cross-sectional area, C_D is a discharge coefficient, P is the pressure, and the subscript throat denotes the choke point (at the orifice, see Section 4.2.1), and the subscript eff denotes effective (after the shock structure and the pressure has returned to atmospheric). These equations are used in several models.

Birch: This formulation is from Birch et al., 1984 [36]. Mass is conserved (Eq. 22 is followed). Steps/assumptions:

- temperature after shock is the stagnation (storage) temperature
- velocity after the shock is sonic ($\text{Ma} = 1$, v_{eff} calculated using Eq. 20 or other thermodynamic relationship)
- conservation of mass from the throat to the after shock conditions determines the diameter

EwanMoodie: Uses the model described by Ewan and Moodie, 1986 [37]. Mass is conserved (Eq. 22 is followed). Steps/assumptions:

- temperature after shock is the throat temperature
- velocity after the shock is sonic ($\text{Ma} = 1$, v_{eff} calculated using Eq. 20 or other thermodynamic relationship)
- conservation of mass from the throat to the after shock conditions determines the diameter

Birch2: This formulation is derived from Birch et al., 1987 [35]. Mass and momentum are conserved. Steps/assumptions:

- temperature after shock is the stagnation (storage) temperature
- velocity of the jet is from the simultaneous solution to the conservation of mass and momentum equations from the throat conditions (Eq. 24 is followed)
- conservation of mass from the throat to the after shock conditions determines the diameter (Eq. 25).

Molkov: Formulation is from Molkov et al., 2009 [38]. Mass and energy are conserved. Steps/assumptions:

- velocity after the shock is sonic ($Ma = 1$, v_{eff} calculated using Eq. 20 or other thermodynamic relationship)
- isentropic expansion from the throat conditions to sonic velocity yields the temperature after the shock

$$h(T_{AS}, P_{AS}) + \frac{1}{2}v_{AS}^2 = h(T_{\text{throat}}, P_{\text{throat}}) + \frac{1}{2}v_{\text{throat}}^2 \quad (26)$$

- conservation of mass from the throat to the after shock conditions determines the diameter (Eq. 22 is followed)

YuceilOtugen: Uses the model described by Yüceil and Ötügen, 2002 [39]. Conserves mass, momentum, and energy. Steps:

- velocity after the shock is determined by the simultaneous solution to the conservation of mass and momentum equations, with temperature determined through isentropic expansion (Eqs. 24 and 26)
- diameter is determined through the conservation of mass (Eq. 25)

HardstadBellan: Uses the model described by Harstad and Bellan, 2006 [40].

4.2.3 Gas Jet/Plume

For a jet or plume of hydrogen, HyRAM follows the one-dimensional model described by Houf and Schefer [41]. While the model only considers one dimension, this dimension is along the streamline, and the jet/plume can curve due to buoyancy effects (or wind, although this feature is not currently included). The reduction in dimension comes from the assumption that the mean

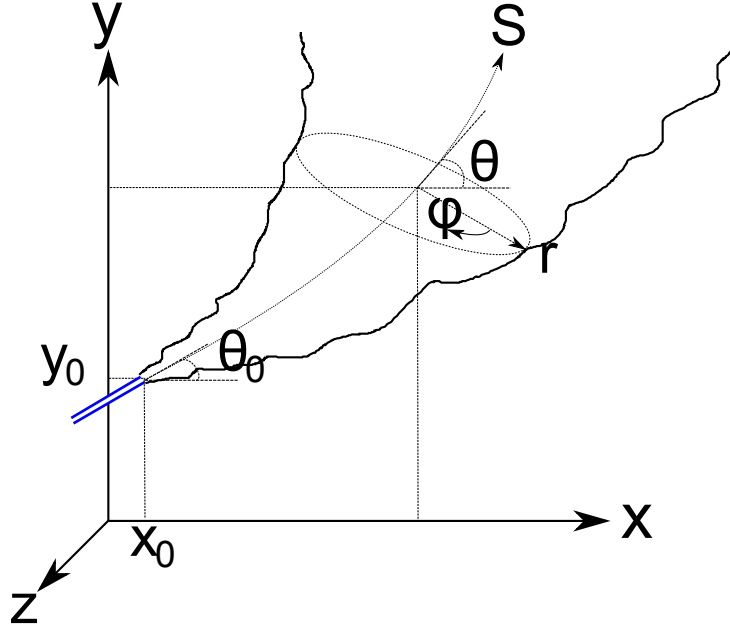


Figure 4. Sketch of plume model coordinates. Gravity acts in the negative y -direction.

profiles of the velocity (v), density (ρ), and product of density and mass fraction (Y) of hydrogen are Gaussian, as

$$v = v_{cl} \exp\left(-\frac{r^2}{B^2}\right) \quad (27)$$

$$\rho = (\rho_{cl} - \rho_{amb}) \exp\left(-\frac{r^2}{\lambda^2 B^2}\right) + \rho_{amb} \quad (28)$$

$$\rho Y = \rho_{cl} Y_{cl} \exp\left(-\frac{r^2}{\lambda^2 B^2}\right), \quad (29)$$

where B is a characteristic half-width, λ is the ratio of density spreading relative to velocity, the subscript cl denotes the centerline, the subscript amb denotes ambient, and r is perpendicular to the stream-wise direction. Gravity acts in the negative y -direction, and the plume angle, θ is relative to the x -axis (horizontal), as shown in Fig. 4. The derivatives of the spatial dimensions are therefore

$$\frac{dx}{dS} = \cos \theta \quad (30)$$

$$\frac{dy}{dS} = \sin \theta. \quad (31)$$

The conservation equations can be written as follows:

continuity:

$$\frac{d}{dS} \int_0^{2\pi} \int_0^\infty \rho v r \, dr \, d\phi = \rho_{amb} E \quad (32)$$

x-momentum:

$$\frac{d}{dS} \int_0^{2\pi} \int_0^\infty \rho v^2 \cos \theta r dr d\phi = 0 \quad (33)$$

y-momentum:

$$\frac{d}{dS} \int_0^{2\pi} \int_0^\infty \rho v^2 \sin \theta r dr d\phi = \int_0^{2\pi} \int_0^\infty (\rho_{amb} - \rho) g r dr d\phi \quad (34)$$

species (hydrogen) continuity:

$$\frac{d}{dS} \int_0^{2\pi} \int_0^\infty \rho v Y r dr d\phi = 0. \quad (35)$$

After plugging in the Gaussian profiles in Eqs. 27-29, a system of first order differential equations can be derived, where the independent variable is S and the dependent variables are v_{cl} , B , ρ_{cl} , Y_{cl} , x , and y , which can be integrated from the starting point to the distance desired. The entrainment model also follows Houf and Schefer [41], where there is a combination of momentum and buoyancy driven entrainment,

$$E = E_{mom} + E_{buoy}, \quad (36)$$

where

$$E_{mom} = 0.282 \left(\frac{\pi D^2}{4} \frac{\rho_{exit} v_{exit}^2}{\rho_\infty} \right)^{1/2} \quad (37)$$

and

$$E_{buoy} = \frac{a}{Fr_l} (2\pi v_{cl} B) \sin \theta, \quad (38)$$

where the local Froude number,

$$Fr_l = \frac{v_{cl}^2}{gD(\rho_\infty - \rho_{cl})/\rho_{exit}}. \quad (39)$$

In these equations, a was empirically determined

$$\begin{cases} a = 17.313 - 0.116665 Fr_{den} + 2.0771 \times 10^{-4} Fr_{den}^2, & Fr_{den} < 268 \\ a = 0.97 & Fr_{den} \geq 268 \end{cases} \quad (40)$$

As the jet/plume becomes very buoyant (as opposed to momentum-dominated), the non-dimensional number

$$\alpha = \frac{E}{2\pi B v_{cl}} \quad (41)$$

will increase. When α reaches the limiting value of $\alpha = 0.082$, α is held constant and the entrainment value becomes

$$E = 2\pi \alpha B v_{cl} = 0.164\pi B v_{cl}. \quad (42)$$

4.2.4 Accumulation in Confined Areas/Enclosures

When a release occurs in an enclosure, a stratified mixture of hydrogen and air can accumulate near the ceiling due to buoyancy.

Jets/plumes are modeled as described in Section 4.2.3. When these releases occur indoors, the plumes could impinge on a wall. Currently, should this impingement happen, the trajectory of the jet/plume is modified such that the hydrogen will travel vertically upwards along the wall, rather than in the horizontal direction, with the same features (e.g. half-width, centerline velocity). Accumulation occurs following the model of Lowesmith et al. [42], where a layer forms along the ceiling. Conservation of mass requires that

$$\frac{dV_l}{dt} = Q_{in} - Q_{out}, \quad (43)$$

where V_l is the volume of gas in the layer, and Q is the volumetric flow rate, with subscript in referring to the flow rate of hydrogen and air entrained into the jet at the height of the layer, and out referring to flow out the ventilation. Species conservation requires that

$$\frac{d(\chi V_l)}{dt} = Q_{leak} - \chi Q_{out}, \quad (44)$$

where χ is the mole or volume fraction of hydrogen in the layer and Q_{leak} is the leak rate of hydrogen. Expanding the derivative and substituting Eq. 43 yields

$$V_l \frac{d\chi}{dt} = Q_{leak} - \chi Q_{in}. \quad (45)$$

Q_{in} is solved for by modeling a jet/plume within the enclosure to calculate the jet half-width (B) and centerline velocity (v_{cl}), as described in Section 4.2.3 at the height of the bottom of the layer. The volumetric flow rate is calculated, Q_{in} , is calculated as $\pi B^2 v_{cl}$. Flows out of the enclosure are driven by buoyancy, and potentially wind or a fan. Buoyancy driven flow is calculated as $Q_B = C_d A_v \sqrt{g' H_l}$, where C_d is a coefficient of discharge, A_v is the area of the vent, H_l is the height of the layer (between the bottom of the layer and the center-point of the outlet vent), and g' is reduced gravity, equal to $g(\rho_{air} - \rho_l)/\rho_{air}$. The density in the layer is calculated from the density of air and the density of hydrogen (at the temperature and pressure of the enclosure) as $\rho_l = \chi \rho_{H_2} + (1 - \chi) \rho_{air}$. Wind is assumed to drive the flow at a rate of $Q_w = C_d A_v U_w / \sqrt{2}$, and the total flow out is calculated as $Q_{out} = \sqrt{Q_B^2 + Q_w^2} + Q_{leak}$.

4.3 Ignited Releases

4.3.1 Jet Flame Without Buoyancy Correction

An engineering correlation developed by Houf and Schefer [25] is used to predict the radiant heat flux from high-pressure turbulent jet-flames. The radiative heat flux at a point is a function of the

transmissivity of the atmosphere between the source and the point, τ , the downstream distance, x , and radial distance from the centerline, r , as

$$q_{\text{rad}}(x, r) = \tau S_{\text{rad}} \frac{C^*}{4\pi r^2}, \quad (46)$$

where S_{rad} is the total emitted radiative power, and C^* is the normalized radiative heat flux, a function of burner diameter, flow rate fuel type, and for turbulent-jet flames, the normalized axial distance. The total emitted radiative power, S_{rad} , is related to the total energy in the flame, and the radiant fraction,

$$S_{\text{rad}} = X_{\text{rad}} \dot{m}_{\text{fuel}} \Delta H_c, \quad (47)$$

where X_{rad} is the radiant fraction, \dot{m}_{fuel} is the mass flow rate of fuel, and ΔH_c is the heat of combustion (118.83 MJ/kg). The radiant fraction (X_{rad}) varies with the flame residence time (τ_f); for hydrogen, the relationship is [43]

$$X_{\text{rad}} = 9.45 \times 10^{-9} (\tau_f a_p T_{\text{ad}}^4)^{0.47}, \quad (48)$$

where a_p is the Planck-mean absorption coefficient for an optically thin flame (0.23 for hydrogen [44]), and T_{ad} is the adiabatic flame temperature (2,390 K for hydrogen [44]). The flame residence time can be calculated as

$$\tau_f = \frac{\rho_f W_f^2 L_{\text{vis}} f_s}{3\rho_j d_j^2 u_j}, \quad (49)$$

where ρ_f , W_f , and L_{vis} are the flame density, width and visible length, f_s is the mass fraction of hydrogen in a stoichiometric mixture of hydrogen and air (0.0283), and ρ_j , d_j , and u_j are the density, diameter, and velocity of the jet at the exit (orifice). The flame density is calculated as the density at the adiabatic flame temperature, $\rho_f = p_{\text{amb}} W_{\text{mix}} / (RT_{\text{ad}})$, where p_{amb} is the ambient pressure, W_{mix} is the mean molecular weight of the stoichiometric products of hydrogen combustion in air, R is the universal gas constant, and T_{ad} is the adiabatic flame temperature. A non-dimensional flame length, defined as

$$L^* = \frac{L_{\text{vis}} f_s}{d_j \sqrt{\rho_j / \rho_{\text{amb}}}}, \quad (50)$$

collapses onto a single curve for a range of fuels (hydrogen, methane, and propane), where

$$L^* = \begin{cases} \frac{13.5 \text{Fr}^{2/5}}{(1+0.07\text{Fr}^2)^{1/5}}, & \text{Fr} < 5, \\ 23, & \text{Fr} > 5. \end{cases} \quad (51)$$

The Froude number (Fr), which is the ratio of buoyancy to momentum forces, is defined as

$$\text{Fr} = \frac{u_j f_s^{3/2}}{\sqrt{g d_j (T_{\text{ad}} - T_{\text{amb}}) / T_{\text{amb}} \sqrt{\rho_j / \rho_{\text{amb}}}}}, \quad (52)$$

where g is the gravitational constant, and T_{amb} is the ambient temperature. The flame width is calculated as $W_f = 0.17 L_{\text{vis}}$. Finally, the normalized radiative heat flux varies as a function of the normalized axial length as

$$C^* = 0.85985 \exp \left(-2.75791 \left| \frac{x}{L_{\text{vis}}} - 0.6352 \right| \right). \quad (53)$$

The transmissivity is calculated, accounting for the absorption from water vapor and CO₂, using a correlation from Wayne [45]:

$$\tau = 1.006 - 0.001171 (\log_{10} X_{\text{H}_2\text{O}}) - 0.02368 (\log_{10} X_{\text{H}_2\text{O}})^2 - 0.03188 (\log_{10} X_{\text{CO}_2}) + 0.001164 (\log_{10} X_{\text{CO}_2})^2, \quad (54)$$

where $X_{\text{H}_2\text{O}}$ and X_{CO_2} is proportional to the amount of water vapor or CO₂ in the path (dimensionless). These values are calculated by $X_{\text{CO}_2} = L \cdot 273/T \cdot c_{\text{CO}_2}/335$ and $X_{\text{H}_2\text{O}} = R_H \cdot L \cdot S_{\text{mm}} \cdot 2.88651 \times 10^{-2}/T$. In these relationships, L is the path length (m) through which the radiative light must travel, T is the ambient temperature (K), c_{CO_2} is the concentration of CO₂ in the atmosphere (ppm – assumed to be 400 ppm), R_H is the fractional relative humidity (ranges from 0 – 1), and S_{mm} is the saturated water vapor pressure (mm Hg), estimated by the relationship, $S_{\text{mm}} = \exp(10.386 - 5132/T)$.

These correlations are used to calculate the radiative heat flux for a straight flame using Eq. 46.

4.3.2 Jet Flame with Buoyancy Correction

A similar model to the jet/plume model described in Section 4.2.3 is also used to describe a flame. The model is described by Ekoto et al. [26]. The major difference between the jet/plume model and the flame model is that rather than the mole fraction, the mixture fraction is a conserved scalar, where for a hydrogen flame, it is defined as

$$f = \frac{MW_{\text{H}_2}(x_{\text{H}_2} + x_{\text{H}_2\text{O}})}{MW} = Y_{\text{H}_2} + Y_{\text{H}_2\text{O}} \frac{MW_{\text{H}_2}}{MW_{\text{H}_2\text{O}}}. \quad (55)$$

Similar assumptions are made for Gaussian profiles:

$$V = V_{cl} \exp\left(-\frac{r^2}{B^2}\right) \quad (56)$$

$$f = f_{cl} \exp\left(-\frac{r^2}{\lambda^2 B^2}\right). \quad (57)$$

And then the conservation equations can be written as

x -centerline:

$$\frac{dx}{dS} = \cos \theta \quad (58)$$

y -centerline:

$$\frac{dy}{dS} = \sin \theta. \quad (59)$$

continuity:

$$\frac{d}{dS} \int_0^{2\pi} \int_0^\infty \rho v r dr d\phi = \rho_{amb} E \quad (60)$$

x-momentum:

$$\frac{d}{dS} \int_0^{2\pi} \int_0^\infty \rho v^2 \cos \theta r dr d\phi = 0 \quad (61)$$

y-momentum:

$$\frac{d}{dS} \int_0^{2\pi} \int_0^\infty \rho v^2 \sin \theta r dr d\phi = \int_0^{2\pi} \int_0^\infty (\rho_{amb} - \rho) g r dr d\phi \quad (62)$$

mixture fraction:

$$\frac{d}{dS} \int_0^{2\pi} \int_0^\infty \rho V f r dr d\phi = 0. \quad (63)$$

Note that energy conservation is not included. The mixture is assumed to be thermally perfect, with the local enthalpy calculated as

$$h = h_{amb} \frac{\rho_{amb}}{\rho} + \Delta H_c (F - Y_{H_2}) \quad (64)$$

Assuming that the mixture is always in equilibrium (neglecting heat-losses), the composition and temperature throughout the flame cross-section can be calculated through Eqs. 55, 57 and 64, using the ideal gas law ($\rho RT = P_{amb} MW$) as an equation of state. From this solution, the density profile, which is not self-similar, can be calculated. Entrainment is once again modeled as the sum of momentum and buoyancy contributions (Eq. 36), but rather than defining the buoyancy caused entrainment as before (Eq. 38), buoyancy driven entrainment is calculated as

$$E_{buoy} = 2\pi \alpha_{buoy} g \sin \theta \frac{\int_0^\infty (\rho_{amb} - \rho) dr}{Bv_{cl} \rho_{exit}}. \quad (65)$$

The empirical constant for momentum driven entrainment in Eq. 37 of 0.282, and empirical constant for buoyancy driven entrainment in Eq. 65 (α_{buoy}) need to be updated for flames rather than unignited plumes/jets, to values of 0.0342, and $\alpha_{buoy} = 5.75 \times 10^{-4}$ [26].

Radiation from a curved flame The radiative heat flux from the buoyancy corrected, curved flame, is similar to that described in Section 4.3.1. However, the flame is broken-up along its length, and a weighted multi-source model, similar to that described by Hankinson and Lowesmith [46] is used to calculate the total heat flux at each point. The heat flux at a point is calculated as

$$q = \tau S_{rad} \frac{V_F}{A_f}, \quad (66)$$

where V_F is the view-factor, proportional to the heat flux transmitted to the observer (similar to C^* in Section 4.3.1), τ is the transmissivity, expressed by a simple Beer-Lambert expression accounting for absorption by the H_2O and CO_2 in the view path, and A_f is the surface area of the flame. Contributions to the total heat flux are broken up into many (N , generally 50) points along the length of the curved flame, and the weighted average proceeds as

$$\tau \frac{V_F}{A_f} = \sum_{i=1}^N \frac{w_i \cos \beta_i}{4\pi D_i^2} \tau_i, \quad (67)$$

where the emitter strength weighting parameter

$$w_i = \begin{cases} iw_1 & i \leq 0.75N \\ \left[n - \frac{n-1}{N-n-1}(i - (n+1)) \right] w_1 & i > 0.75N \end{cases}, \quad (68)$$

with the constraint that $1 \leq n \leq N$ and $\sum_{i=1}^N w_i = 1$. In these equations, D and β are the distance and angle, respectively between the observer and unit normal to the point emitter, and the transmissivity at each point, τ , is calculated using Eq. 54.

4.3.3 Overpressure in Enclosures

If a confined mixture ignites, significant overpressures can develop within the enclosure or confinement area.

Overpressure is calculated assuming that the cause of overpressure is the volume change on combustion pressurizing the enclosure⁵. It is assumed that all of the hydrogen above the lower flammability limit (in both the jet/plume and the accumulated layer) reacts, and the overpressure is calculated, following Bauwens and Dorofeev [47] as

$$\Delta p = p_0 \left(\left[\left(\frac{V_T + V_{H_2}}{V_T} \right) \left(\frac{V_T + V_{stoich}(\sigma - 1)}{V_T} \right) \right]^\gamma - 1 \right), \quad (69)$$

where p_0 is the initial pressure, V_T is the total volume of the enclosure, V_{H_2} is the expanded volume of pure hydrogen following the release, V_{stoich} is the volume of a stoichiometric mixture of the consumed hydrogen, σ is the expansion ratio of a stoichiometric hydrogen-air mixture, and γ is the specific heat ratio of air. The expanded volume is given by $V_{H_2} = m_{H_2}/\rho_{H_2}$ where m_{H_2} is the mass of hydrogen consumed and ρ_{H_2} is the density of hydrogen at ambient conditions. V_{stoich} is V_{H_2} divided by the stoichiometric mole fraction of hydrogen.

⁵Note that this approach is different than the overpressure calculations based on the blast wave in unconfined mixtures.

5 Mathematics Middleware

This section describes additional functionality created or leveraged to reliably implement the algorithms described elsewhere in this report and to provide additional user features.

5.1 The Math.NET Numerics Package

HyRAM uses the Math.NET Numerics package provided under the MIT/X11 License [48]. This package provides methods and algorithms for numerical computations in science and engineering. Math.NET Numerics provides a mature library of well-known and widely accepted state-of-the-art algorithm implementations that are thoroughly tested, consistently named and ready to use. Topics include special functions, linear algebra, probability models, random numbers, interpolation, integration, regression, optimization problems and more. Because this library is open-source, algorithm verification can be performed by any interested party.

The Math.NET Numerics functionality currently being leveraged from within HyRAM includes items from its Distribution module (Math.NET.Numerics.Distribution). HyRAM currently uses the following user-selectable probability distributions from this module: Normal, Lognormal, Beta and Uniform. Because standard descriptions of these distributions are widely available and their operation as implemented within the Math.NET library is consistent with such descriptions, they are not described here. All of the distributions implement a common set of operations such as evaluating the density and the cumulative distribution at a given point, or computing the mean and standard deviation, along with other properties. Technical information about these distributions can be found in the package documentation [49].

The HyRAM QRA algorithm calls the Math.NET distributions for several models, including release frequency (Section 2.4) and both thermal and overpressure harm models (Section 2.6). In most cases, the user is able to specify the distribution being performed on the input, and uncertain input is requested from Math.NET Numerics without requiring additional code.

5.2 The HyRAM Unit Conversion System

HyRAM enforces an immutable link between values and the units that define them. Input values are stored in the International System of Units (SI). The only way to retrieve or set values is by specifying a compatible unit when submitting or retrieving data from the session database. This is important from a quality and code-readability standpoint: Wherever data is set or retrieved, the unit used is plainly visible.

Conversions are performed implicitly by the system. Therefore, the application is able to present data in units preferred by the user or more relevant in problem context, while being able to pass data to the provider algorithm in units expected by the algorithm or function call. Inside middleware and implicit behind a low-level API, simple unit conversion is enabled by specifying

a conversion factor, which is applied as the data is stored or retrieved. A conversion delegate is created and applied when more complicated conversion is called for or application of a conversion factor is inadequate. When software algorithms are called by HyRAM, the correct (expected) unit representation is always used.

All model inputs are stored internal to HyRAM, in data structures defining and exposing the HyRAM session database. Each individual value (array, ordinal or complex data type) is stored in an executable class called a convertible value node that facilitates database storage and unit-independent treatment of data. Each node encapsulates data setting and retrieval operations, aggregating a set of unit of measurement converters, member functions for setting and retrieving values and member variables defining and enforcing the valid range of values.

Consumers of HyRAM data use the GetValue and SetValue member routines from the containing convertible value node instance to get and set values. The first argument passed to these routines identifies the unit type. The next argument (or result as appropriate) is the actual value, represented in the specified unit of measurement.

Table 5.2 contains the convertible units currently available in HyRAM. Additional units of measurement will be added to HyRAM as needed. The user is able to change the unit of measurement being used while viewing or changing inputs. These values are converted and redisplayed automatically.

Table 5. HyRAM Convertible Units

Unit Type	Units Available
Distance	m, cm, mm, ft, in, yd, mi, au
Area	m ² , cm ² , mm ² , ft ² , in ² , yd ²
Volume	cm ³ , dm ³ , m ³ , km ³ , mm ³ , μ m ³ , ft ³ , in ³ , yd ³ , L, μ L, mL, dL, kL, ML
Angle	radians, degrees
Energy	J, kWh, BTU
Time	s, ms, min, hr
Pressure	Pa, kPa, MPa, psi, psig, atm, bar
Temperature	Celsius, Fahrenheit, Kelvin
Speed	m/s

6 Summary of Numerical Methods

Many of the physics simulations used by HyRAM require numerical solutions to the mathematical equations as they are too difficult or impossible to analytically compute the solution. The Python physics modules take advantage of the numerical methods implemented in Python's NumPy and SciPy packages [50]. NumPy provides support for multi-dimensional arrays, mathematical functions of arrays, and some numerical linear algebra routines. SciPy provides a variety of numerical method routines including support for numerical linear algebra, integration, interpolation, optimization, rootfinding, ordinary differential equation (ODE) solvers, etc. as well as support for sparse matrices. Both Numpy and Scipy are open source, BSD-licensed, well-documented, well-tested and highly optimized, often written in C or calling optimized BLAS or LAPACK routines.

This section describes which numerical methods are used for the various physics modules. This focuses on the primary methods used for the major physics computations. Other numerical methods are used as needed, such as nonlinear equation solvers. Also, many of the modules build on one another. The methods themselves are not described here in detail. For a detailed description of the methods, the authors recommend consulting any of the standard numerical analysis/scientific computing textbooks or the NumPy/SciPy documentation for the method. Note that this section is only relevant to the Physics modules; the appropriate methods and tools used for the QRA computations are described in Section 5.

6.1 Equation of State Computations

The majority of the equation of state equations were analytically solved for the appropriate variable and then the resulting expressions for the desired variables are simply evaluated. In a few cases, however, the equations were either too difficult or impossible to solve analytically. In these instances, an appropriate numerical method for rootfinding is used.

6.2 Notional Nozzle Model Computations

Determining the throat conditions utilizes the equation of state computations. Then, the majority of the computations for the notional nozzles just require evaluation of certain expressions. However, in a couple of instances, appropriate numerical methods for rootfinding from SciPy are utilized.

6.3 Unignited Gas/Jet Plume

Solving for the jet plume involves utilizing the relevant equation of state and notional nozzle computations. The primary aspect of calculating the jet plume is integrating the system of ordinary differential equations (ODEs) resulting from the conservation equations (described in Section 4.2.3).

To integrate the system of ODEs, the jet plume physics module uses SciPy’s built in ODE integrator with the “dopri5” integrator. This (“dopri5”) is an explicit Runge-Kutta method of order (4)5. Each step of the ODE integration (evaluating the governing equations) requires solving a system of linear equations. This is a small linear system that is solved using a direct solver from NumPy which uses the LU decomposition with partial pivoting.

6.4 Jet Flame

Similar to the jet plume, the jet flame also utilizes the relevant equation of state and notional nozzle computations. As with the jet plume, the major computation of the jet flame is the integration of the system of ODEs resulting from the conservation equations. This is also integrated using the same ODE integrator from SciPy with “dopri5”, the explicit Runge-Kutta method of order (4)5. For the jet flame, each step of the ODE integration (evaluating the governing equations) consists of two primary numerical methods. First, spatial integration from 0 to ∞ with respect to r is performed using the composite trapezoid rule. Then, the resulting system of equations is solved using a NumPy’s direct solver which uses the LU decomposition with partial pivoting.

Additionally, other miscellaneous computations are also required for plotting, computing radiative heat flux, etc. that make use of numerical methods. These numerical methods include numerical differentiation, interpolation, and rootfinding.

6.5 Overpressure

To compute the overpressure, the jets/plumes are computed as described in Section 4.2.3 using the methods described in Section 6.3. The system of ODEs resulting from the conservation equations described in Section 4.2.4 is integrated with the ODE integrator in SciPy with “dopri5”, an explicit Runge-Kutta method of order (4)5. In addition to the integration of the system of ODEs resulting from the conservation equations, various other numerical methods including interpolation, rootfinding, etc. are used to compute specific quantities, such as using interpolation to determine the pressure at the user specified times.

7 Engineering Toolkit

This section describes additional functionality created or leveraged to reliably implement the algorithms described elsewhere in this report and to provide additional user features.

7.1 Temperature, Pressure, and Density

The user can calculate one of these quantities (temperature (T), pressure (P), or density (ρ)) by specifying the other two. The algorithm uses the Abel-Noble equation of state [51].

$$P = \frac{(\rho R_{H_2} T)}{(1 - b\rho)} = Z\rho R_{H_2} T \quad (70)$$

Where $Z = \frac{1}{(1-b\rho)}$ is the compressibility factor, b is the co-volume constant, and R_{H_2} is the gas constant for hydrogen ($R_{H_2} = 4.12 \text{ N m/ gm K}$). Z is unity for an ideal gas ($b = 0$), and Abel-Noble converges to the ideal gas law at low pressures (below 172 bar) for hydrogen.

7.2 Tank Mass

The user can calculate the mass (M) of hydrogen in a container by specifying the temperature (T), pressure (P), and volume (V) of the container.

$$M = \rho V \quad (71)$$

Where the density, ρ , is calculated with the Abel-Noble equation of state described in the above section.

7.3 Mass Flow Rate

The mass flow rate (\dot{m}) of a leak from a tank can be calculated for either a steady release or for a pressure blowdown of a tank. (A “blowdown” describes the release of gas from a tank until the pressure reaches ambient, causing the mass flow to stop.) The user must specify the temperature (T), pressure (P), and leak size (“Orifice Diameter”, d) for a steady release, and also volume (V) for a blowdown case.

For the blowdown case, the total mass in the tank is calculated with

$$M = \rho V \quad (72)$$

The change in mass (d_{mass}) for a given number of steps (n_{steps} is hard coded to 1,000), is calculated with

$$d_{mass} = \frac{M}{n_{steps}} \quad (73)$$

The initial mass flow rate is calculated from the initial conditions of the tank and leak. Then a time step size is calculated with

$$d_t = \frac{d_{mass}}{\dot{m}} \quad (74)$$

The mass in the tank (M) is then solved for at each time step

$$M = M - \dot{m}d_t \quad (75)$$

as well as the new thermodynamic conditions in the tank and the new mass flow rate from those conditions. This is iterated until the pressure in the tank equals the ambient pressure (101,325 Pa). The output for the steady state case is the mass flow rate in kg/s and for the blowdown case is a plot of the mass flow rate vs time.

7.4 TNT Mass Equivalence

The user can calculate the TNT mass equivalence by specifying the flammable vapor release mass (m_{fuel}), the explosive energy yield, Y (in %, from 0 to 100), and the net heat of combustion (ΔH_c). This is calculated as:

$$m_{TNT \text{ equivalent}} = \frac{m_{fuel} \times Y \times \Delta H_c}{4500 \text{ kJ/kg}_{TNT}}. \quad (76)$$

Units may be selected by the user. Note that the heat of combustion for hydrogen is $\Delta H_{c, \text{hydrogen}} = 118,830 \text{ kJ/kg}$.

References

- [1] K. M. Groth and A. V. Tchouvelev, “A toolkit for integrated deterministic and probabilistic risk assessment for hydrogen infrastructure,” in *Proceedings of the International Conference on Probabilistic Safety Assessment and Management (PSAM 12)*, Honolulu, HI, 22–27 June 2014.
- [2] A. V. Tchouvelev, K. M. Groth, P. Benard, and T. Jordan, “A hazard assessment toolkit for hydrogen applications,” in *Proceedings of the 20th World Hydrogen Energy Conference (WHEC 2014)*, 2014.
- [3] K. M. Groth and E. S. Hecht, “HyRAM: A methodology and toolkit for quantitative risk assessment of hydrogen systems,” in *In Proceedings of the International Conference on Hydrogen Safety (ICHS 2015)*, Yokohama, Japan, October 19-21 2015.
- [4] H. R. Zumwalt and K. M. Groth, “HyRAM V1.0 user’s manual,” Sandia National Laboratories, Albuquerque, NM, SAND2015-7380 R, August 2015.
- [5] J. T. Reynolds, “HyRAM testing strategy and quality design elements,” Sandia National Laboratories, Albuquerque, NM, SAND2014-20676, December 2014.
- [6] J. M. Ohi, C. Moen, J. Keller, and R. Cox, “Risk assessment for hydrogen codes and standards,” in *Proceedings of the first International Conference on Hydrogen Safety, (ICHS 2005)*, 2005, pp. 8–10.
- [7] J. LaChance, W. Houf, B. Middleton, and L. Fluer, “Analyses to support development of risk-informed separation distances for hydrogen codes and standards,” Sandia National Laboratories, Albuquerque, NM, SAND2009-0874, March 2009.
- [8] J. LaChance, “Risk-informed separation distances for hydrogen refueling stations,” *International Journal of Hydrogen Energy*, vol. 34, no. 14, pp. 5838–5845, 2009.
- [9] J. LaChance, A. Tchouvelev, and J. Ohi, “Risk-informed process and tools for permitting hydrogen fueling stations,” *International Journal of Hydrogen Energy*, vol. 34, no. 14, pp. 5855–5861, 2009.
- [10] J. L. LaChance, B. Middleton, and K. M. Groth, “Comparison of NFPA and ISO approaches for evaluating separation distances,” *International Journal of Hydrogen Energy*, vol. 37, no. 22, pp. 17 488–17 496, November 2012.
- [11] K. M. Groth, J. L. LaChance, and A. P. Harris, “Early-stage quantitative risk assessment to support development of codes and standard requirements for indoor fueling of hydrogen vehicles,” Sandia National Laboratories, Albuquerque, NM, SAND2012-10150, November 2012.
- [12] —, “Design-stage QRA for indoor vehicular hydrogen fueling systems,” in *Proceedings of the European Society for Reliability Annual Meeting (ESREL 2013)*, Amsterdam, September 29 - October 2 2013, pp. 2247–2256.

- [13] H. J. Pasman, “Challenges to improve confidence level of risk assessment of hydrogen technologies,” *International Journal of Hydrogen Energy*, vol. 36, no. 3, pp. 2407–2413, 2011.
- [14] K. Groth and A. Harris, “Hydrogen quantitative risk assessment workshop proceedings,” Sandia National Laboratories, Albuquerque, NM, SAND2013-7888, August 2013.
- [15] K. Ham, A. Marangon, P. Middha, N. Versloot, N. Rosmuller, M. Carcassi, O. R. Hansen, M. Schiavetti, E. Papanikolaou, A. Venetsanos, A. Engebø, J. L. Saw, J.-B. Saffers, A. Flores, and D. Serbanescu, “Benchmark exercise on risk assessment methods applied to a virtual hydrogen refuelling station,” *International Journal of Hydrogen Energy*, vol. 36, no. 3, pp. 2666–2677, 2011.
- [16] A. Kotchourko, D. Baraldi, P. Benard, N. Eisenreich, T. Jordan, J. Keller, A. Kessler, J. LaChance, V. Molkov, M. Steen, A. Tchouvelev, and J. Wen, “State of the art and research priorities in hydrogen safety,” Joint Research Centre of the European Commission (JRC), , 2014.
- [17] A. V. Tchouvelev, “Risk assessment studies of hydrogen and hydrocarbon fuels, fuelling stations: Description and review,” International Energy Agency Hydrogen Implementing Agreement Task 19, , 2006.
- [18] Center for Chemical Process Safety (CCPS), *Guidelines for Chemical Process Quantitative Risk Analysis*. American Institute of Chemical Engineers, 1999.
- [19] T. Aven, *Foundations of risk analysis*. John Wiley & Sons, 2003.
- [20] M. Modarres, *Risk Analysis in Engineering: Techniques, Tools, and Trends*. CRC Press, 2006.
- [21] SFPE, “SFPE engineering guide to performance-based fire protection analysis and design of buildings,” National Fire Protection Association, Quincy, MA, USA, , 2007.
- [22] S. E. Rose, S. Flamberg, and F. Leverenz, *Guidance Document for Incorporating Risk Concepts into NFPA Codes and Standards*. Fire Protection Research Foundation, March 2007.
- [23] J.-E. Vinnem, *Offshore Risk Assessment: Principles, Modelling and Applications of QRA Studies*, 2nd ed. Springer, 2007.
- [24] T. Aven, *Quantitative risk assessment: the scientific platform*. Cambridge University Press, 2011.
- [25] W. Houf and R. Schefer, “Predicting radiative heat fluxes and flammability envelopes from unintended releases of hydrogen,” *International Journal of Hydrogen Energy*, vol. 32, no. 1, pp. 136–151, 2007.
- [26] I. W. Ekoto, A. J. Ruggles, L. W. Creitz, and J. X. Li, “Updated jet flame radiation modeling with buoyancy corrections,” *International Journal of Hydrogen Energy*, vol. 39, no. 35, pp. 20 570–20 577, Dec. 2014.

- [27] J. LaChance, A. Tchouvelev, and A. Engebø, "Development of uniform harm criteria for use in quantitative risk analysis of the hydrogen infrastructure," *International Journal of Hydrogen Energy*, vol. 36, no. 3, pp. 2381–2388, 2011.
- [28] N. A. Eisenberg, C. J. Lynch, and R. J. Breeding, "Vulnerability model. A simulation system for assessing damage resulting from marine spills," U. S. Coast Guard, SA/A-015 245, 1975.
- [29] C. K. Tsao and W. W. Perry, "Modifications to the vulnerability model: a simulation system for assessing damage resulting from marine spills," U. S. Coast Guard, ADA 075 231, 1979.
- [30] TNO, "Methods for the determination of possible damage," The Netherlands Organization of Applied Scientific Research (TNO), CPR 16E, 1992.
- [31] F. P. Lees, "The assessment of major hazards: a model for fatal injury from burns," *Process safety and environmental protection*, vol. 72, no. 3, pp. 127–134, 1994.
- [32] HSE, *Major hazard aspects of the transport of dangerous substances*. UK Health and Safety Executive (HSE), 1991.
- [33] E. Lemmon, M. Huber, and M. McLinden, "NIST standard reference database 23: Reference fluid thermodynamic and transport properties - REFPROP, Version 9.1," National Institute of Standards and Technology, Standard Reference Data Program, Gaithersburg, MD, , 2013.
- [34] J. W. Leachman, R. T. Jacobsen, S. G. Penoncello, and E. W. Lemmon, "Fundamental equations of state for parahydrogen, normal hydrogen, and orthohydrogen," *Journal of Physical and Chemical Reference Data*, vol. 38, no. 3, pp. 721–748, 2009.
- [35] A. D. Birch, D. J. Hughes, and F. Swaffield, "Velocity decay of high pressure jets," *Combustion Science and Technology*, vol. 52, no. 1-3, pp. 161–171, 1987.
- [36] A. D. Birch, D. R. Brown, M. G. Dodson, and F. Swaffield, "The structure and concentration decay of high pressure jets of natural gas," *Combustion Science and Technology*, vol. 36, no. 5-6, pp. 249–261, 1984.
- [37] B. C. R. Ewan and K. Moodie, "Structure and velocity measurements in underexpanded jets," *Combustion Science and Technology*, vol. 45, no. 5-6, pp. 275–288, 1986.
- [38] V. Molkov, D. Makarov, and M. Bragin, "Physics and modelling of under-expanded jets and hydrogen dispersion in atmosphere," in *Proceedings of the 24th international conference on interaction of intense energy fluxes with matter*, March 1-6 2009.
- [39] K. B. Yüceil and M. V. Ötügen, "Scaling parameters for underexpanded supersonic jets," *Physics of Fluids*, vol. 14, no. 12, pp. 4206–4215, 2002.
- [40] K. Harstad and J. Bellan, "Global analysis and parametric dependencies for potential unintended hydrogen-fuel releases," *Combustion and Flame*, vol. 144, no. 12, pp. 89 – 102, 2006.
- [41] W. Houf and R. Schefer, "Analytical and experimental investigation of small-scale unintended releases of hydrogen," *International Journal of Hydrogen Energy*, vol. 33, no. 4, pp. 1435–1444, 2008.

- [42] B. Lowesmith, G. Hankinson, C. Spataru, and M. Stobbart, "Gas build-up in a domestic property following releases of methane/hydrogen mixtures," *International Journal of Hydrogen Energy*, vol. 34, no. 14, pp. 5932–5939, July 2009.
- [43] P. P. Panda and E. S. Hecht, "Ignition and flame characteristics of cryogenic hydrogen releases," *International Journal of Hydrogen Energy*, vol. 42, no. 1, pp. 775–785, 2017.
- [44] A. Molina, R. W. Schefer, and W. G. Houf, "Radiative fraction and optical thickness in large-scale hydrogen-jet fires," *Proc. Combust. Inst.*, vol. 31, no. 2, pp. 2565–2572, Jan. 2007.
- [45] F. D. Wayne, "An economical formula for calculating atmospheric infrared transmissivities," *Journal of Loss Prevention in the Process Industries*, vol. 4, no. 2, pp. 86 – 92, 1991.
- [46] G. Hankinson and B. J. Lowesmith, "A consideration of methods of determining the radiative characteristics of jet fires," *Combust. Flame*, vol. 159, no. 3, pp. 1165–1177, 2012.
- [47] C. Bauwens and S. Dorofeev, "CFD modeling and consequence analysis of an accidental hydrogen release in a large scale facility," *International Journal of Hydrogen Energy*, vol. 39, no. 35, pp. 20 447–20 454, Dec. 2014.
- [48] Math.net numerics. [Online]. Available: <http://numerics.matdotnet.com>
- [49] Probability distributions. Math.NET Numerics. [Online]. Available: <http://numerics.matdotnet.com>
- [50] S. van der Walt, S. C. Colbert, and G. Varoquaux, "The numpy array: A structure for efficient numerical computation," *Computing in Science Engineering*, vol. 13, no. 2, pp. 22–30, March 2011.
- [51] R. W. Schefer, W. Houf, T. C. Williams, B. Bourne, and J. Colton, "Characterization of high-pressure, underexpanded hydrogen-jet flames," *International Journal of Hydrogen Energy*, vol. 32, no. 12, pp. 2081–2093, 2007.

DISTRIBUTION:

- 1 Charles (Will) James Jr, PhD
U.S. Department of Energy
Office of Energy Efficiency & Renewable Energy
Fuel Cell Technologies Office
Safety, Codes, and Standards
1000 Independence Avenue, SW
Washington, DC 20585
- 1 MS 0736 Richard O. Griffith, 6230
- 1 MS 0748 Katrina Groth, 6231
- 1 MS 0748 Brian D. Ehrhart, 6231
- 1 MS 0748 Cathy Ottinger Farnum, 6231
- 1 MS 0748 Chris B. LaFleur, 6231
- 1 MS 0748 Alice B. Muna, 6231
- 1 MS 0748 F. Mitch McCrory, 6231
- 1 MS 0748 John T. Reynolds, 9341
- 1 MS 9052 Ethan Hecht, 8367
- 1 MS 9053 Isaac Ekoto, 8362
- 1 MS 9161 Chris San Marchi, 8367
- 1 MS 9161 Jonathan A. Zimmerman, 8367
- 1 MS 9957 Myra L. Blaylock, 8253
- 1 MS 9957 Patricia E. Gharagozloo, 8253
- 1 MS 0899 Technical Library, 9536 (electronic copy)

